DD-OOK Multicore Fiber Systems Impaired by Intercore Crosstalk and Laser Phase Noise

Tiago M. F. Alves, Adolfo V. T. Cartaxo, and João L. Rebola

***Abstract*—Direct-detection on-off keying (DD-OOK) weakly-coupled multicore fiber (WC-MCF) systems impaired by intercore crosstalk (ICXT) and laser phase noise are investigated numerically and experimentally. This is performed for systems with a product between the bit rate and the absolute value of the skew between cores much larger than one. It is shown that the phase noise increases the instantaneous ICXT power fluctuations. The standard deviation of the short-term average ICXT (STAXT) power induced by the phase noise depends on the product between the laser linewidth and the absolute value of the skew between cores (linewidth$\times$|skew|). When linewidth$\times$|skew|$\gg$1, typical of distributed feedback (DFB) lasers (linewidth in the few MHz range) and MCFs with skew in the μs range, the decrease of the standard deviation of the STAXT power induced by the phase noise is 5 dB per decade of linewidth$\times$|skew| increase. For linewidth$\times$|skew|$\ll$1, typical of external cavity lasers (ECLs) and DFB lasers, and MCFs with skew of a few ns, the standard deviation of the STAXT power remains almost unaffected by the phase noise. Experimental results show that, compared with low linewidth ECLs, 10 Gb/s DD-OOK WC-MCF systems using DFB lasers as optical sources in the interfering cores and skew in the range between 2.4 ns and 5.4 ns, may require an additional ICXT margin up to 8 dB for a given outage probability. The additional ICXT margin and the lower amplitude of the STAXT power fluctuations observed experimentally for DFB lasers suggest that the level of the fluctuations of the STAXT power may be an inadequate system performance indicator. The dependence of the outage probability on the interfering core count is also investigated experimentally. It is shown that, for systems with bit rate$\times$|skew|$\gg$1, the outage probability only depends on the total ICXT power and not on the interfering core count.**

***Index Terms*—Data centers, intercore crosstalk, laser phase noise, multicore fiber, on-off keying, short reach networks, space division multiplexing.**

I. Introduction

Multicore fiber (MCF) technology has potential to provide a high increase of the capacity provisioning in next-generation optical networks [1]–[5]. MCFs can be categorized into weakly-coupled (WC) and strongly-coupled fibers. Compared with strongly-coupled MCFs, WC-MCFs generate low mean intercore crosstalk (ICXT) power levels and, in combination with intensity modulation/direct detection (IM-DD) systems, are a good candidate for short reach networks where the cost is a primary concern [6], [7].

The authors are with the Lisbon site of Instituto de Telecomunicações, 1049-001 Lisbon, Portugal. The authors are also with Iscte - Instituto Universitário de Lisboa, Portugal. e-mail: tiago.alves@lx.it.pt.

This work was supported in part by Fundação para a Ciência e a Tecnologia (FCT) from Portugal under the internal projects of Instituto de Telecomunicações DigCore/UIDP/50008/2020 and UIDB/EEA/50008/2020.

Due to the core density increase, required to reduce the system cost and maximize the transmission capacity, the ICXT power increases and can become an important impairment in WC-MCF based networks. Several models have been proposed to characterize the ICXT [8]–[15]. Most models are focused on the ICXT randomness along the longitudinal direction of the MCF and rely on two different principles: (i) the randomness is continuously distributed along the MCF [8]–[12], or (ii) the randomness is lumped at discrete points along the MCF [13]–[15]. Compared with the former, the lumped modelling provides an efficient and simple tool to numerically emulate the ICXT at the expense of some inaccuracy in application scenarios where the phase matching region does not exist [15]. The original discrete changes model (DCM) includes only randomness along the longitudinal direction of the fiber [13] and does not describe the random variation of the short term average ICXT (STAXT) along time and frequency observed experimentally in [16], [17]. The STAXT is defined as the average ICXT power measured at the output of the interfered core by an optical power meter along a very short time interval ($\approx$100 ms). The main ideas of the DCM are: (i) the ICXT field induced by the interfering core at the output of the interfered core results from a sum of N_p contributions associated with N_p phase-matching points (PMPs) (PMPs: points along the longitudinal coordinate of the MCF for which the difference between the effective refractive indexes of the interfering and interfered cores is zero), and (ii) each one of these contributions is weighted by a random phase shift (RPS), due to the effect of slight random fluctuations of the MCF structure. In order to improve the ICXT modelling, the original DCM was generalized to include: (i) the difference between the dispersion parameters of the cores [18]; (ii) the real homogeneous WC-MCFs, i. e. WC-MCFs whose cores have similar but not exactly the same refractive indexes [15]; (iii) the dependence on the modulation frequency [16]; (iv) the dual-polarization [19], (v) the random variation of the ICXT over time [20], [21]; and (vi) the dependence of the ICXT on the optical frequency [22]. The numerical implementation of this generalized DCM enabled to show that: (i) for long monitoring periods, the ICXT polarization state varies significantly along time [23], as reported experimentally in [24], and (ii) the random fluctuations of the ICXT over time and frequency may lead to time periods in which very high ICXT peak power levels occur and, therefore, to time intervals with possible service unavailability [25], [26], which has been also confirmed experimentally [27]. With carrier-free signals, the ICXT power fluctuations can be relieved by using MCFs with high skew-bit rate product. In signals containing a

strong optical carrier, like on-off keying (OOK), a high level of ICXT fluctuations occurs even for large skew and symbol rates [28]. Preliminary simulation results using the DCM have also shown that the combined effect of the ICXT and laser phase noise can significantly affect the received eye-pattern and outage probability of 10 Gb/s OOK WC-MCF systems [29]. In DD orthogonal frequency division multiplexing systems, photodetected ICXT power variations induced by phase noise that exceed 20 dB have been observed with a time duration scale that is much shorter than the scale of the time variation typical of ICXT mechanism [17]. More recently, it was shown that the choice of the light source used for the STAXT measurements has significant impact on their precision [30].

In this work, the impact of the laser phase noise on the instantaneous ICXT power, on the STAXT power and on the performance of DD-OOK WC-MCF systems is studied. In particular, the impact of the product between the laser linewidth and the skew between cores on the STAXT and outage probability is investigated by simulation and experimentally. This work is an extension of [31].

II. Theory: Impact of Laser Phase Noise on the ICXT Power

From the dual polarization DCM, the slowly varying complex amplitude of the electric field of the interfered core n at the MCF output normalized by the core loss, $\mathbf{E}_n(L,t) = [E_{n,x}(L,t)\ \ E_{n,y}(L,t)]^T$, induced by core m, can be written as [21]:

$$\mathbf{E}_n(L,t) = C\times \times \sum_{k=1}^{N_p} \begin{bmatrix} v_{1,n,m}^{(k)}(t) & v_{2,n,m}^{(k)}(t) \\ v_{3,n,m}^{(k)}(t) & v_{4,n,m}^{(k)}(t) \end{bmatrix} \begin{bmatrix} F_{n,m}^{(k)}\left(0, t-\overline{\xi}_{n,m}^{(k)}\right) \\ F_{n,m}^{(k)}\left(0, t-\overline{\xi}_{n,m}^{(k)}\right) \end{bmatrix} \quad (1)$$

where L is the MCF length, t is the time and $C = \frac{\overline{K}_{n,m}}{2j}$. $\overline{K}_{n,m}$=$0.5\left(\overline{K}_{n,m,x} + \overline{K}_{n,m,y}\right)$ is the discrete coupling coefficient given by the average of the intercore coupling coefficients (between cores n and m) of the two orthogonal polarization directions $\mathbf{u_x}$ and $\mathbf{u_y}$. Equation 1 considers the power at the input of the m-th interfering core equally split between the polarization directions, random coupling between polarizations and linear propagation along the WC-MCF, and

$$v_{i,n,m}^{(k)}(t) = \exp\left[-j(\Phi_{i,m}^{(k)}(t) + \overline{\phi}_{n,m}^{(k)})\right], \quad 1 \le i \le 4 \quad (2)$$

$$F_{n,m}^{(k)}(0,t) = \mathcal{F}^{-1}\left[\tilde{E}_m(0,\omega)\exp\left(-j\overline{\eta}_{n,m}^{(k)}\omega^2\right)\right] \quad (3)$$

$$\overline{\phi}_{n,m}^{(k)} = \overline{\beta}_{n,0}\left(L - z_m^{(k)}\right) + \overline{\beta}_{m,0} z_m^{(k)} \quad (4)$$

$$\overline{\xi}_{n,m}^{(k)} = \overline{\beta}_{n,1}\left(L - z_m^{(k)}\right) + \overline{\beta}_{m,1} z_m^{(k)} \quad (5)$$

$$\overline{\eta}_{n,m}^{(k)} = 0.5\left[\overline{\beta}_{n,2}\left(L - z_m^{(k)}\right) + \overline{\beta}_{m,2} z_m^{(k)}\right] \quad (6)$$

where ω is the angular frequency, $\mathcal{F}^{-1}$ is the inverse Fourier transform operator, $\tilde{E}_m(0,\omega)$ is the Fourier transform of the slowly varying complex amplitude of the electric field of the m-th interfering core at the MCF input and $z_m^{(k)}$ is the longitudinal coordinate of the MCF corresponding to the k-th center point between consecutive PMPs of core m. $\overline{\beta}_{q,0}$ is the average of the intrinsic propagation constant of core q of the two polarizations at zero frequency. $\overline{\beta}_{q,i}$ (with i=1 or i=2) are the average of the i-th order derivative of the intrinsic propagation constant of core q (with q=m or q=n) of the two polarizations with respect to angular frequency, which are the inverse of the group velocity and the group velocity dispersion of core q, respectively. The functions $v_{i,n,m}^{(k)}(t)$ represent the coupling between different (with i=2 and i=3) and the same (with i=1 and i=4) polarization directions [19], [20]. $\Phi_{i,m}^{(k)}(t)$ are independent random processes that represent the contributions of the time varying nature of the RPS associated with each PMP of the m-th interfering core to the Jones vector of the ICXT field. Independent RPS for the different polarization directions are considered. With this, the ICXT fields induced in the interfered core n in the two polarization directions are uncorrelated. The instantaneous ICXT power at the interfered core output is given by $p(t) = |E_{n,x}(L,t)|^2 + |E_{n,y}(L,t)|^2$.

To get theoretical insight on the influence of the laser phase noise on the instantaneous ICXT power, we neglect the impact of the phase shift accumulated at zero frequency, given by $\overline{\phi}_{n,m}^{(k)}$, and the group velocity dispersion of the fiber on the ICXT field. We consider also the complex amplitude of the electric field of the m-th interfering core at the MCF input given by $E_m(0,t)$=$s(t)\exp(j\Phi_L(t))$, with $\Phi_L(t)$ the phase noise of the laser field and $s(t)$ the modulated signal at the interfering core input. In this case, the two components of the ICXT field given in Eq. 1 can be approximated by:

$$E_{n,x}(L,t) \approx C\sum_{k=1}^{N_p}\left[\exp\left(-j\Phi_{1,m}^{(k)}(t)\right) + \exp\left(-j\Phi_{2,m}^{(k)}(t)\right)\right] \times s\left(t-\overline{\xi}_{n,m}^{(k)}\right)\exp\left(j\Phi_L\left(t-\overline{\xi}_{n,m}^{(k)}\right)\right) \quad (7)$$

$$E_{n,y}(L,t) \approx C\sum_{k=1}^{N_p}\left[\exp\left(-j\Phi_{3,m}^{(k)}(t)\right) + \exp\left(-j\Phi_{4,m}^{(k)}(t)\right)\right] \times s\left(t-\overline{\xi}_{n,m}^{(k)}\right)\exp\left(j\Phi_L\left(t-\overline{\xi}_{n,m}^{(k)}\right)\right) \quad (8)$$

The random variation of the ICXT field along time expressed in Eq. 7 (or Eq. 8) is affected mainly by three distinct effects. (i) The ICXT mechanism, modelled by the stochastic RPSs, $\Phi_{i,m}^{(k)}(t)$, and characterized by the ICXT decorrelation time, with typical values in MCFs ranging from a couple of minutes to a couple of hours [16], [21]. (ii) The modulated signal launched into the interfering core, characterized by the bit or symbol period with time scale on the ps range for typical data rates above 10 Gb/s. (iii) The phase noise, $\Phi_L(t)$, induced by the laser source used to inject the signal in the interfering core, that is characterized by the coherence time of the laser field.

The coherence time, defined as $t_c = 1/(\pi \times \Delta\nu)$ with $\Delta\nu$ the laser linewidth, provides information about the time interval over which the laser field is correlated: (i) the phases of the laser field at different time instants whose difference is within the coherence time have some degree of correlation; (ii) if the time difference exceeds the coherence time, the phases are weakly correlated or uncorrelated. External cavity lasers

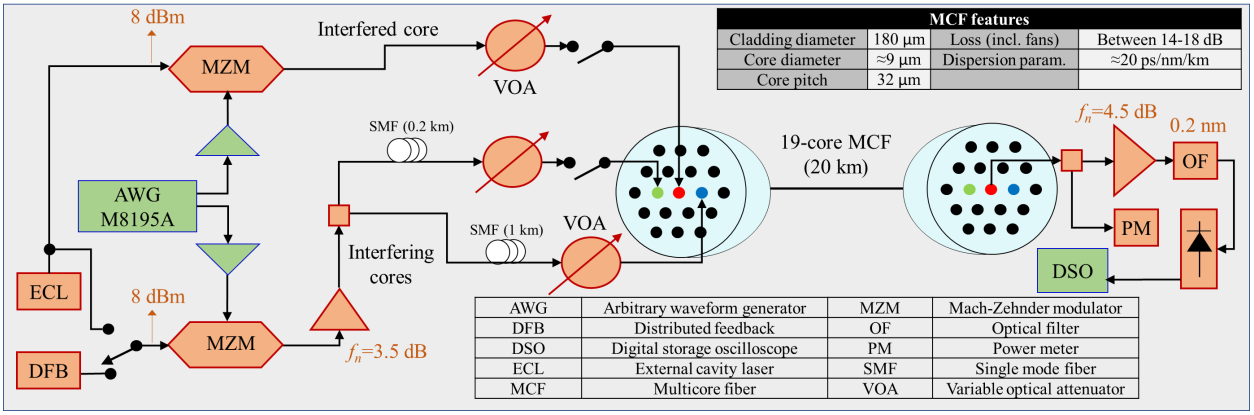

Fig. 1. Setup employed to assess the impact of the combined effect of the laser phase noise and ICXT in WC-MCF based DD-OOK systems.

(ECLs) and distributed feedback (DFB) lasers are characterized by a coherence time on the μs and ns scale, respectively. Eq. 7 and Eq. 8 show that the impact of the laser phase noise on the ICXT field is also affected by the delay, $\overline{\xi}_{n,m}^{(k)}$, that is proportional to the relative propagation time delay between cores n and m, i. e., the skew. As a reference, so far, in short length MCFs developed targeting research activities, the skew between cores is typically in the ns range [16], [21], [32].

Let us now consider the case in which the skew is much shorter than the time interval over which the laser field is correlated. This is the typical case of systems operating with low linewidth ECLs. In this case, linewidth$\times$|skew|$\ll$1, and the time delay induced in the phase noise terms of Eq. 7 and Eq. 8 can be approximated by $\overline{\beta}_{n,1}L$. Thus, the ICXT field induced in core n can be approximated by:

$$E_{n,x}(L,t) \approx C\exp\left(j\Phi_L\left(t-\overline{\beta}_{n,1}L\right)\right)\times \times\sum_{k=1}^{N_p}\left[\exp\left(-j\Phi_{1,m}^{(k)}(t)\right)+\exp\left(-j\Phi_{2,m}^{(k)}(t)\right)\right]s\left(t-\overline{\xi}_{n,m}^{(k)}\right) \quad (9)$$

$$E_{n,y}(L,t) \approx C\exp\left(j\Phi_L\left(t-\overline{\beta}_{n,1}L\right)\right)\times \times\sum_{k=1}^{N_p}\left[\exp\left(-j\Phi_{3,m}^{(k)}(t)\right)+\exp\left(-j\Phi_{4,m}^{(k)}(t)\right)\right]s\left(t-\overline{\xi}_{n,m}^{(k)}\right) \quad (10)$$

From Eq. 9 and Eq. 10, the instantaneous ICXT power is given by:

$$\begin{aligned} p(t) &= |E_{n,x}(L,t)|^2+|E_{n,y}(L,t)|^2 = \\ &= |C|^2\left|\sum_{k=1}^{N_p}\left[\exp\left(-j\Phi_{1,m}^{(k)}(t)\right)+\exp\left(-j\Phi_{2,m}^{(k)}(t)\right)\right]\times\right. \\ &\left.\times\, s\left(t-\overline{\xi}_{n,m}^{(k)}\right)\right|^2+ \\ &+|C|^2\left|\sum_{k=1}^{N_p}\left[\exp\left(-j\Phi_{3,m}^{(k)}(t)\right)+\exp\left(-j\Phi_{4,m}^{(k)}(t)\right)\right]\times\right. \\ &\left.\times\, s\left(t-\overline{\xi}_{n,m}^{(k)}\right)\right|^2 \end{aligned} \quad (11)$$

Equation 11 shows that, for systems with linewidth$\times$|skew|$\ll$1, the instantaneous ICXT power induced at the output of the interfered core is independent of the laser phase noise. Thus, as the time variation of the ICXT mechanism is in the minutes range, the time variation of the instantaneous ICXT power in systems with linewidth$\times$|skew|$\ll$1 should be similar to that of the modulated signal, $s(t)$.

If the skew is not much shorter than the time interval over which the laser field is correlated, i. e., systems where linewidth$\times$|skew|$\gtrsim$1 and particularly linewidth$\times$|skew|$\gg$1, we cannot further simplify the ICXT field given by Eq. 7 and Eq. 8. In this case, the instantaneous ICXT power is given by:

$$\begin{aligned} p(t) &= \\ &= |C|^2\left|\sum_{k=1}^{N_p}\left[\exp\left(-j\Phi_{1,m}^{(k)}(t)\right)+\exp\left(-j\Phi_{2,m}^{(k)}(t)\right)\right]\times\right. \\ &\left.\times\, s\left(t-\overline{\xi}_{n,m}^{(k)}\right)\exp\left(j\Phi_L\left(t-\overline{\xi}_{n,m}^{(k)}\right)\right)\right|^2+ \\ &+|C|^2\left|\sum_{k=1}^{N_p}\left[\exp\left(-j\Phi_{3,m}^{(k)}(t)\right)+\exp\left(-j\Phi_{4,m}^{(k)}(t)\right)\right]\times\right. \\ &\left.\times\, s\left(t-\overline{\xi}_{n,m}^{(k)}\right)\exp\left(j\Phi_L\left(t-\overline{\xi}_{n,m}^{(k)}\right)\right)\right|^2 \end{aligned} \quad (12)$$

From Eq. 12, we conclude that the instantaneous ICXT power in systems with linewidth$\times$|skew|$\gtrsim$1 may be significantly affected by the laser phase noise. This occurs because many contributions of the ICXT originated along the MCF to the optical field at the interfered core output are further uncorrelated or weakly correlated due to the phase noise. Eq. 12 shows also that the time scale of the instantaneous ICXT power variation in systems with linewidth$\times$|skew|$\gtrsim$1 is dominantly impaired by the combined effect of the modulated signal and laser phase noise.

Previous work has shown that, in the absence of laser phase noise, the mean of the instantaneous ICXT power is given by $N_p|\overline{K}_{nm}^2|$ [21]. From Eq. 12, it can be shown that the mean of the instantaneous ICXT power in phase noise impaired systems is also given by $N_p|\overline{K}_{nm}^2|$, regardless the laser linewidth value. Further conclusions on the impact of

the combined effect of the laser phase noise and ICXT on the system performance when linewidth$\times$|skew|$\gtrsim$1, particularly linewidth$\times$|skew|$\gg$1, are difficult to be drawn from the theoretical expressions due to the algebra complexity. In the following sections, the analysis of this case is performed using numerical simulation and experimentally.

III. System Setup

In this section, the setup used to analyze the impact of the laser phase noise on the ICXT and system performance by numerical simulation and experimentally is described. The setup is shown in Fig. 1 and represents a 10 Gb/s DD-OOK WC-MCF system. Experiments with one and two interfering cores in a 20-km long weakly-coupled homogeneous 19-core MCF are performed. In numerical simulations, only one interfering core is considered.

The experiments are performed with an HP8168F external cavity laser (ECL) with a narrow linewidth of 100 kHz and an off-the-shelf JDSU distributed feedback (DFB) laser with linewidth in the MHz range. The 10 Gb/s OOK waveform comprises 2^{14} bits and is generated by a 60 Gsamples/s Keysight M8195A. Electrooptic conversion is realized by a 10 GHz Mach-Zehnder modulator (MZM) with extinction ratio of 10 dB. In order to decorrelate the signals launched in the interfered and interfering cores, spools of standard single-mode fiber with 0.2 km and 1 km are used at the interfering cores input. To emulate a MCF with ultra high core count, the power launched into the interfered and interfering cores is adequately chosen to have the system performance dominantly impaired by ICXT. In all experiments, the central core (core 1) is used as the interfered core. The skew between cores is 5.4 ns for cores (1,2), and 2.4 ns for cores (1,5). For core numbering, please see [21]. With this, the skew-bit rate product is much higher than one which is preferable from the performance viewpoint in carrier-assisted systems [27]. The ICXT decorrelation time of cores (1,2) and (1,5) is 3.4 minutes and 2.8 minutes, respectively [21]. At the output of the interfered core, the STAXT power induced by the OOK signal is monitored by a power meter. For STAXT power measurements (performed, in this work, with modulated data in the interfering core), the optical switch at the input of the interfered core is open. The ICXT-impaired OOK signal is then optically amplified, photodetected and captured by a 20 Gsamples/s real-time oscilloscope. Offline processing with digital filtering (4th-order Bessel low-pass filter with 8 GHz bandwidth) and error counting are performed. The STAXT power and bit error ratio (BER) were monitored continuously over several days in a temperature-controlled room environment. The MZM biases were also monitored periodically to assure stable and reliable setup measurements.

The setup used for numerical simulation is equivalent to that of Fig. 1. The Matlab plataform is used for simulation and custom scripts are developed to describe the different system blocks. The phase noise introduced by the continuous wave laser is modeled by a Wiener process with zero mean and variance of $t\Delta\nu/(2\pi)$ for $t>0$. Each realization of the laser phase noise and modulated signal are generated from the beginning of the first time fraction (at t=0) until the end of the last time fraction. However, only the signal waveforms generated in the time interval corresponding to each time fraction are used in the analysis. The MCF simulation considers group velocity dispersion, skew between cores and the dual polarization ICXT model [21]. To focus the attention on the combined effect of laser phase noise and intercore crosstalk, fiber nonlinearities and polarization mode dispersion are not considered in this work. The dual polarization ICXT model considers that the random fluctuations of the polarization and the random evolution of the ICXT along time are induced by RPSs associated with each PMP. The RPSs are modelled by independent Wiener processes with the ICXT decorrelation time set to five minutes. The evolution of the RPSs along time is generated using different seeds for different RPSs. Each time fraction, with duration of 3.3 μs, consists of a sequence of 2^{15} bits. The frequency resolution is 30 kHz enabling a good spectral description of the laser field associated with the phase noise process. The STAXT power is evaluated over hundreds of time fractions (time interval between fractions is 5 minutes) to adequately characterize the STAXT stochastic features. The time interval between time fractions should be compared with the decorrelation time of the ICXT to provide some information about the correlation of the ICXT generated in adjacent time fractions. For instance, if the time interval between time fractions is much lower than the ICXT decorrelation time, approximately the same mean ICXT power in a significant number of time fractions is observed and, thus, a similar system performance is expected in those time fractions. Contrarily, if the time interval between time fractions is much longer than the ICXT decorrelation time, then adjacent time fractions are affected by uncorrelated ICXT. In this case, significant differences on the system performance may be expected for different time fractions.

IV. Results and Discussion

A. Simulation Results

In this subsection, the impact of the laser phase noise on the ICXT power is assessed by numerical simulation. Only two cores of the MCF are considered in this subsection. To illustrate the impact of the laser phase noise effect on the time waveform of the instantaneous ICXT power or STAXT power, the RPSs of the ICXT mechanism are the same when lasers with different linewidths are assessed. The ICXT level, defined as the ratio between the mean ICXT power and mean signal power at the output of interfered core, is close to -28 dB.

Figure 2 shows the evolution of the STAXT power along the time. The STAXT power is induced by a 10 Gb/s OOK signal (interfering core) and is calculated at the output of the interfered core. The STAXT power is evaluated at each five minutes (time interval between time fractions), considering: (i) an ideal laser (linewidth of 0 Hz), i. e., with the system being impaired only by the ICXT effect, and (ii) a laser with linewidth of 10 MHz (typical of DFB lasers) where the combined effect of laser phase noise and ICXT is assessed. The skew between cores is 100 ns to better illustrate the impact of the laser phase noise on the STAXT power. The results of

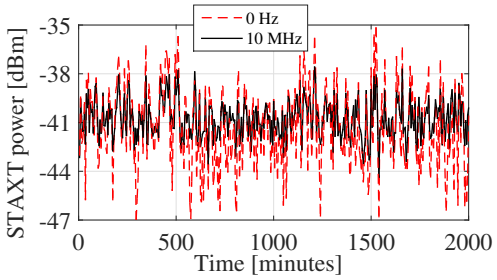

Fig. 2. Evolution of the STAXT power along time obtained by simulation for an ideal laser and a laser with linewidth of 10 MHz.

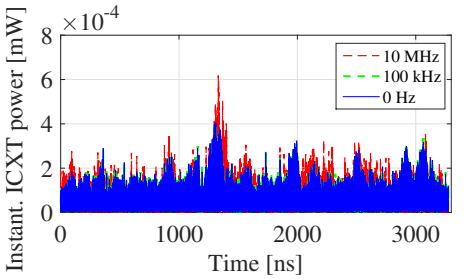

(a)

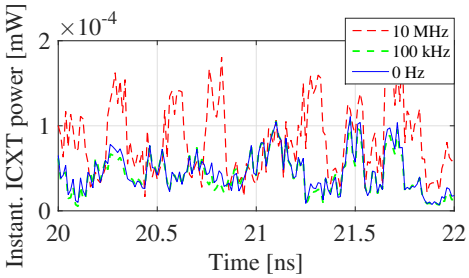

(b)

Fig. 3. (a) Instantaneous ICXT power obtained by simulation as a function of the time in a specific time fraction for different laser linewidths. (b) Zoom of (a).

Fig. 2 suggest that the combined effect of laser phase noise and ICXT may significantly reduce the fluctuations of the STAXT power.

Figure 3(a) depicts the instantaneous ICXT power as a function of time for a given time fraction. Fig. 3(b) shows a zoom of Fig. 3(a). Note that the RPSs of the ICXT mechanism are the same for the three cases analyzed in Fig. 3, i. e., the three curves of Fig. 3 would be overlapped if the phase noise effect was neglected. The analysis of Figure 3 suggests that the fluctuations of the instantaneous ICXT power along the time fraction increase when the laser linewidth (and, thus, when the phase noise variance) increases. As the fluctuations of the instantaneous ICXT power are random, they should be characterized statistically. For this reason, we evaluated the standard deviation of the instantaneous ICXT power fluctuations shown in Fig. 3(a). Compared with the ideal laser, the standard deviation of the instantaneous ICXT power fluctuations for lasers with 100 kHz and 10 MHz, is 0.1 dB and 1.1 dB higher, respectively. Figure 3(b) shows that the fluctuations of the instantaneous ICXT power present a time scale that is of the order of the bit period (0.1 ns), which agrees with

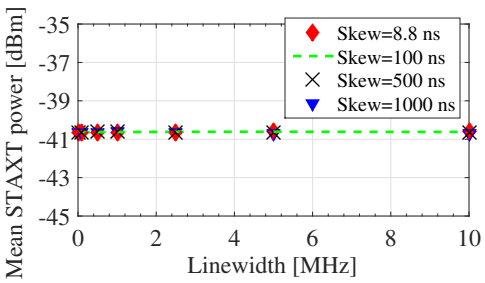

Fig. 4. Mean of the STAXT power obtained by simulation as a function of the laser linewidth.

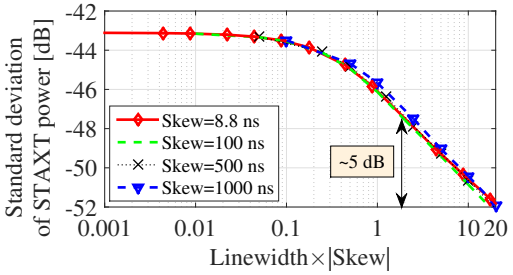

Fig. 5. Standard deviation of the STAXT power obtained by simulation as a function of the product between the laser linewidth and the skew.

the discussion of the time scale variation of the instantaneous ICXT power presented in section II. Figure 3(b) shows also that the amplitude of the fluctuations are significantly higher for lasers with linewidth of 10 MHz than with 100 kHz. This occurs due to the weak correlation or uncorrelation induced by the phase noise on the contributions of the ICXT originated along the MCF to the optical field at the interfered core output.

Despite the fluctuations of the instantaneous ICXT power increase with the laser phase noise, lasers with larger linewidths are less likely of having significant differences between the average ICXT power calculated over two different time fractions due to the averaging effect. Thus, the STAXT, that averages the instantaneous ICXT power over a time interval much longer than the bit duration, tends to present fluctuations with lower amplitude, as suggested by Fig. 2. In simulation, the averaging is performed over each time fraction with duration of 3.3 μs. In experiments, it is performed over the integration time of the power meter.

Fig. 4 depicts the mean of the STAXT power as a function of the laser linewidth. Results for several skews are presented. For each linewidth, the mean of the STAXT power is evaluated over 400 time fractions. Figure 4 shows that the mean of the STAXT power is neither affected by the laser phase noise nor by the skew. The STAXT power in each time fraction, shown in Fig. 2, is evaluated by averaging the instantaneous ICXT power along the time fraction. The mean STAXT power, shown in Fig. 4, is evaluated by averaging the STAXT power over all the time fractions. This is the same as evaluating the mean of the instantaneous ICXT power along a long time period (much longer than the time fraction duration) which is independent of the laser linewidth, as discussed in subsection II.

Figure 5 depicts the standard deviation of the STAXT power

as a function of the product between the laser linewidth and the skew between cores. For each linewidth×|skew|, the standard deviation is evaluated over 400 time fractions. For linewidth×|skew|≪1, the decrease of the standard deviation of the STAXT power is negligible (≪1dB). This occurs because, with linewidth×|skew|≪1, the ICXT power is weakly affected by the laser phase noise, as shown in section II. For the pair of cores used in the experiments, with a skew of 2.4 ns and 5.4 ns, the decrease of the standard deviation of the STAXT power predicted by Fig. 5 is 0.1 dB and 0.3 dB, respectively, when the laser linewidth increases from 0 Hz to 10 MHz. When linewidth×|skew|≈ 1, the decrease of the standard deviation of the STAXT power, relative to linewidth×|skew|≪1, is 3 dB. When linewidth×|skew|≫1, the decrease of the standard deviation of the STAXT power is close to 5 dB per decade of linewidth×|skew| increase. As explained in section II, the impact of the phase noise on the fluctuations of the STAXT power when linewidth×|skew|≫1 occurs because the skew is much higher than the time interval over which the laser field is correlated and, therefore, the different contributions of the ICXT originated along the MCF to the optical field at the interfered core output are further decorrelated by the phase noise.

B. Experimental Results

In this section, the impact of the laser phase noise on the STAXT power and performance of 10 Gb/s OOK systems is assessed experimentally. We stress that the results of STAXT power were obtained by injecting modulated data on the interfering core.

Figure 6(a) depicts the evolution of the STAXT power along time when either the ECL or the DFB laser are used to generate the signal injected into the interfering core. Figure 6(b) shows a zoom of Fig. 6(a). The results, shown in Fig. 6 when the ECL or the DFB laser are employed, were obtained in an interleaved fashion. The time interval between successive measurements captured with the ECL and the DFB laser does not exceed 90 seconds, which is lower than the ICXT decorrelation time. The experimental results of Fig. 6 suggest that the amplitude of the fluctuations of the STAXT obtained with the ECL are, in most of the time, higher than with the DFB laser. Further investigation have also shown that the mean of the STAXT power depicted in Fig. 6(a) is the same for the two lasers, in agreement with the simulation results of Fig. 4. Figure 6(b) shows that, despite the higher amplitude of the fluctuations of the STAXT power obtained with the ECL relative to the DFB laser, the two curves of the STAXT power follow a similar variation along the time. This occurs because the time interval between ECL and DFB laser measurements is lower than the ICXT decorrelation time and, therefore, the measurements with ECL and DFB laser are affected approximately by the same strength of the ICXT mechanism. As a consequence, the variation of the STAXT power along the time induced by the ICXT mechanism is small.

Histograms of the STAXT power depicted in Fig. 6(a), normalized by the mean of the STAXT power evaluated over the monitoring period, for the two laser sources have been

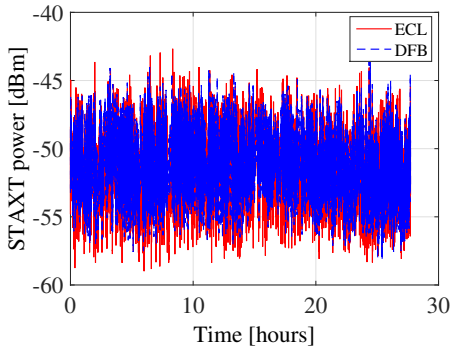

(a)

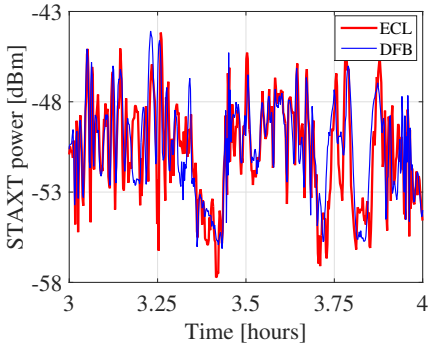

(b)

Fig. 6. (a) Experimental results of the evolution of the STAXT power along time when the ECL or DFB laser is employed as optical source in the interfering core. (b) Zoom of (a).

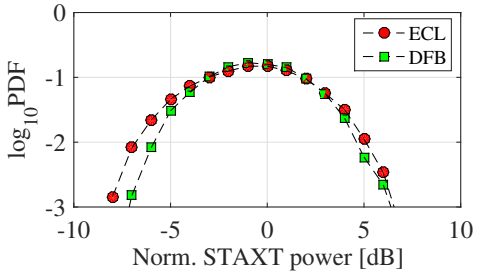

Fig. 7. Histograms of experimental results of the normalized STAXT power when the ECL or DFB laser is employed as optical source in the interfering core.

also obtained. The histograms are shown in Fig. 7 and confirm that the STAXT power fluctuations decrease when lasers with higher linewidths are used. A 0.4 dB decrease between the standard deviation of the STAXT power measured with the ECL and the DBF laser is observed, which agrees well with the simulation results of subsection IV-A. The behaviour of the standard deviation of the STAXT power shown in Fig. 5 should still be further validated experimentally for linewidth×|skew|≳1. That validation is not performed in this work because adequate equipment is not available in our lab.

To investigate the impact of the laser source on the system performance, the BER of the 10 Gb/s bit stream was monitored experimentally. As low BER levels are obtained in most of the time and worse BER events, induced by high ICXT powers,

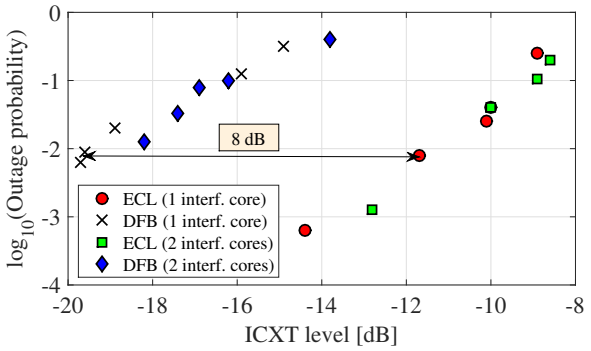

Fig. 8. Experimental results of the outage probability of the OOK signal as a function of the total ICXT level when the ECL or DFB lasers are employed as optical sources in the interfering cores.

occur sporadically [27], [33], the performance of these systems should be characterized using the outage probability, i. e., the probability that the BER exceeds a given BER threshold. In this work, the outage probability was calculated from the experimental BER measurements captured day after day along several months and considering a pre-FEC BER threshold of 1.5×10^{-2}=$10^{-1.82}$ (20.5% FEC). To assure stable and reliable setup BER measurements along the long monitoring period, the setup was deployed in a temperature-controlled room environment and the MZM biases were monitored periodically. The relative polarization between signal and ICXT was not controlled in the experiment to emulate a real system operation. Each BER value used to calculate the outage probability was estimated when 100 errored bits occur, at least. This means that the time required to obtain the outage probabilities for the different ICXT levels shown in Fig. 8 ranged between a few hours to one or two weeks.

Figure 8 depicts the outage probability of the OOK signal obtained experimentally as a function of the total ICXT level, considering one (core 5) and two (cores 2 and 5) adjacent interfering cores. ECL or DFB lasers are employed as optical sources in the interfering cores. The optical source of the interfered core is the ECL in order to have negligible performance degradation induced by the phase-to-intensity noise conversion along fiber propagation [34], [35]. The results of Fig. 8 show that 10 Gb/s DD-OOK MCF systems operating with DFB lasers may require an additional ICXT margin of about 8 dB relative to systems operating with low linewidth ECLs. This worse outage probability observed for lasers with larger linewidths happens because the occurrence of errors on the OOK bit stream received in each time fraction depends on the instantaneous ICXT. As the increase of the laser phase noise variance leads to the increase of the instantaneous ICXT power fluctuations, higher ICXT power levels are more likely to occur and the BER threshold is surpassed more times. Figure 8 shows also that, for the same total ICXT level, the outage probability is similar for systems with one or two interfering cores. This is in agreement with simulation results presented in [36], where it has been concluded that, for systems with bit rate$\times$|skew|$\gg$1, the maximum acceptable total ICXT level from multiple cores for a given outage probability is practically independent of the interfering core count.

The results of section IV suggest that, for DD-OOK WC-MCF systems with bit rate$\times$|skew|$\gg$1, the performance is inadequately characterized by the level of the STAXT power fluctuations. This occurs because the STAXT and outage probability are differently affected by the laser phase noise: (i) a decrease of the STAXT power fluctuations induced by the increase of the laser phase noise variance is observed, and (ii) when the laser phase noise variance increases, the outage probability suffers from additional degradation caused by the larger fluctuations of the instantaneous ICXT power.

V. Conclusion

DD-OOK WC-MCF systems impaired by the combined effect of the laser phase noise and ICXT have been investigated numerically and experimentally for bit rate$\times$|skew|$\gg$1. It has been shown that the STAXT and outage probability are differently affected by the laser phase noise and that the level of the fluctuations of the STAXT power may be an inadequate metric to qualitatively characterize the system performance. When the laser phase noise variance increases: (i) for linewidth$\times$|skew|$\gg$1, the decrease of the standard deviation of the STAXT power fluctuations is close to 5 dB per decade of increase of linewidth$\times$|skew|, due to the STAXT averaging effect; and (ii) the fluctuations of the instantaneous ICXT power increase and the outage probability suffers from additional degradation caused by these larger ICXT fluctuations. For bit rate$\times$|skew|$\gg$1, DD-OOK WC-MCF systems operating with DFB lasers may require an additional ICXT margin up to 8 dB relative to ECL-based systems. It has been also shown that the outage probability only depends on the total ICXT power level and not on the interfering core count.

References

[1] D. Richardson, J. Fini, and L. Nelson, "Space-division multiplexing in optical fibres," *Nat. Photon.*, vol. 7, pp. 354-362, 2013.

[2] Z. Feng, B. Li, M. Tang, L. Gan, R. Wang, R. Lin, Z. Xu, S. Fu, L. Deng, W. Tong, S. Long, L. Zhang, H. Zhou, R. Zhang, S. Liu, and P. Shum, "Multicore-fiber-enabled WSDM optical access network with centralized carrier delivery and RSOA-based adaptive modulation," *Photon. J.*, vol. 7, no. 4, pp. 7201309, 2015.

[3] J. Galvé, I. Gasulla, S. Sales, and J. Capmany, "Reconfigurable radio access networks using multicore fibers," *J. Quantum Electron.*, vol. 52, no. 1, pp. 0600507, 2011.

[4] D. Butler, M. Li, S. Li, Y. Geng, R. Khrapko, R. Modavis, V. Nazarov, and A. Koklyushkin, "Space division multiplexing in short reach optical interconnects," *J. Lightw. Technol.*, DOI 10.1109/JLT.2016.2619981, 2017.

[5] S. Beppu, M. Kikuta, K. Igarashi, H. Mukai, M. Shigihara, Y. Saito, D. Soma, H. Takahashi, N. Yoshikane, I. Morita, M. Suzuki, and T. Tsuritani, "Real-time transoceanic coupled 4-core fiber transmission," *Proc. of Optical Fibre Communication Conference*, paper F3B.4, San Francisco, USA, 2021.

[6] T. Hayashi, T. Nagashima, T. Morishima, Y. Saito and T. Nakanishi, "Multi-core fibers for data center applications," *Proc. of European Conference on Optical Communications*, DOI: 10.1049/cp.2019.0754, 2019.

[7] S. Le, K. Schuh, F. Buchali, T. Drenski, A. Hills, M. King and T. Sizer, "Optical single-sideband direct detection transmissions: recent progress and commercial aspects," *Proc. of European Conference on Optical Communications*, DOI:10.1109/ECOC48923.2020.9333386, 2020.

[8] M. Koshiba, K. Saitoh, K. Takenaga, and S. Matsuo, "Analytical expression of average power-coupling coefficients for estimating intercore crosstalk in multicore fibers," *Photon. J.*, vol. 4, no. 5, pp. 1987–1995, Oct. 2012.

[9] A. Macho, C. Meca, F. Pelaez, M. Morant, and R. Llorente, "Birefringence effects in multi-core fiber: coupled local-mode theory," *Optics Express*, vol. 24, no. 19, pp. 21415-21434, 2016.

[10] S. Mumtaz, R. Essiambre, and G. Agrawal, "Nonlinear propagation in multimode and multicore fibers: generalization of the Manakov equations," *J. Lightw. Technol.*, vol. 31, no. 3, pp. 398–406, 2013.

[11] A. Cartaxo and J. Morgado, "New expression for evaluating the mean crosstalk power in weakly-coupled multi-core fibers," *J. Lightw. Technol.*, vol. 39, no. 6, pp. 1830–1842, 2021.

[12] C. Antonelli, G. Riccardi, T. Hayashi, and A. Mecozzi, "Role of polarization-mode coupling in the crosstalk between cores of weakly-coupled multi-core fibers," *Optics Express*, vol. 28, no. 9, pp. 12847–12861, 2020.

[13] T. Hayashi, T. Nagashima, O. Shimakawa, T. Sasaki, and E. Sasaoka, "Crosstalk variation of multi-core fibre due to fibre bend," *Proc. of European Conference on Optical Communications*, paper We.8.F.6, Torino, Italy, 2010.

[14] T. Hayashi, T. Taru, O. Shimakawa, T. Sasaki, and E. Sasaoka, "Design and fabrication of ultra-low crosstalk and low-loss multi-core fiber," *Optics Express*, vol. 19, no. 17, pp. 16576-16592, 2011.

[15] A. Cartaxo and T. Alves, "Discrete changes model of inter-core crosstalk of real homogeneous multi-core fibers," *J. Lightwave Technol.*, DOI: 10.1109/JLT.2017.2652067, 2017.

[16] R. Luís, B. Puttnam, A. Cartaxo, W. Klaus, J. Mendinueta, Y. Awaji, N. Wada, T. Nakanishi, T. Hayashi, and T. Sasaki, "Time and modulation frequency dependence of crosstalk in homogeneous multi-core fibers," *J. Lightwave Technol.*, vol. 34, no. 2, pp. 441-447, 2016.

[17] T. Alves, A. Cartaxo, R. Luís, B. Puttnam, Y. Awaji, and N. Wada, "Intercore crosstalk in direct-detection homogeneous multicore fiber systems impaired by laser phase noise," *Optics Express*, vol. 25, no. 23, pp. 29417-29431, 2017.

[18] A. Cartaxo, R. Luís, B. Puttnam, T. Hayashi, Y. Awaji, and N. Wada, "Dispersion impact on the crosstalk amplitude response of homogeneous multi-core fibers," *Photon. Technol. Lett.*, vol. 28, no. 17, pp. 1858-1861, Sep. 2016.

[19] R. Soeiro, T. Alves, and A. Cartaxo, "Dual polarization discrete changes model of inter-core crosstalk in multi-core fibers," *Photon. Technol. Lett.*, vol. 29, no. 16, pp. 1395-1398, 2017.

[20] T. Alves and A. Cartaxo, "Inter-core crosstalk in homogeneous multi-core fibers: theoretical characterization of stochastic time evolution," *J. Lightwave Technol.*. vol. 35, no. 21, pp. 4613-4623, 2017.

[21] T. Alves and A. Cartaxo, "Characterization of the stochastic time evolution of short-term average intercore crosstalk in multicore fibers with multiple interfering cores," *Optics Express*, vol. 26, no. 4, pp. 4605-4620, 2018.

[22] T. Alves and A. Cartaxo, "Decorrelation bandwidth of intercore crosstalk in weakly coupled multicore fibers with multiple interfering cores," *J. Lightwave Technol.*, vol. 37, no. 3, pp. 744-754, 2019.

[23] A. Cartaxo, T. Alves, and J. Rebola, "Review of the discrete changes model of intercore crosstalk in weakly-coupled multicore fibers," *Proc. of International Conf. on Transparent Optical Networks*, pp. 1-4, DOI: 10.1109/ICTON51198.2020.9203180, 2020.

[24] G. Rademacher, R. Luís, B. Puttnam, Y. Awaji, and N. Wada, "Crosstalk-induced system outage in intensity modulated direct-detection multi-core fiber transmission," *J. Lightwave Technol.*, DOI: 10.1109/JLT.2019.2945654, 2020.

[25] B. Puttnam, R. Luís, T. Eriksson, W. Klaus, J. Mendinueta, Y. Awaji, and N. Wada, "Impact of intercore crosstalk on the transmission distance of QAM formats in multicore fibers," *Photon. J.*, vol. 8, no. 2, pp. 0601109, 2016.

[26] J. Rebola, T. Alves, A. Cartaxo, and A. Marques, "Outage probability due to intercore crosstalk in dual-core fiber links with direct-detection," *Photon. Technol. Lett.*, DOI: 10.1109/LPT.2019.2921934, 2019.

[27] T. Alves, A. Cartaxo, and J. Rebola, "Stochastic properties and outage in crosstalk-impaired OOK-DD weakly-coupled MCF applications with low and high skew×bit-rate," *J. Sel. Topics Quantum Electron.*, vol. 26, no. 4, pp. 4300208, 2020.

[28] G. Rademacher, R. Luís, B. Puttnam, Y. Awaji, and N. Wada, "Crosstalk dynamics in multi-core fibers," *Optics Express*, vol. 25, no. 10, pp. 12020-12028, 2017.

[29] J. Rebola, T. Alves, and A. Cartaxo, "Assessment of the combined effect of laser phase noise and intercore crosstalk on the outage probability of DD OOK systems," *Proc. of International Conference on Transparent Optical Networks*, paper WeD1.4, Angers, France, 2019.

[30] R. Luís, G. Rademacher, B. Puttnam, Y. Awaji, and N. Wada, "Experimental evaluation of the impact of the light source on the measurement of short-term average crosstalk in homogeneous single-mode multi-core fibers," *Optics Express*, vol. 28, no. 23, pp. 35099-35107, 2020.

[31] T. Alves, J. Rebola, and T. Alves, "Weakly-coupled MCF direct-detection OOK systems impaired by laser phase noise," *Proc. of Optical Fibre Communication Conference*, paper W7B.2, San Francisco, USA, 2021.

[32] B. Puttnam, G. Rademacher, R. Luís, J. Sakaguchi, Y. Awaji, and N. Wada, "Inter-core skew measurements in temperature controlled multi-core fiber," *Proc. of Optical Fibre Communication Conference*, paper Tu3B.3, San Diego, USA, 2018.

[33] T. Alves, J. Rebola, and A. Cartaxo, "Outage probability due to intercore crosstalk in weakly-coupled MCF systems with OOK signaling," *Proc. of Optical Fibre Communication Conference*, paper M2I.1, San Diego, USA, 2019.

[34] S. Yamamoto, N. Edagawa, H. Taga, Y. Yoshida, and H. Wakabayashi, "Analysis of laser phase noise to intensity noise conversion by chromatic dispersion in intensity modulation and direct detection optical fiber transmission," *J. Lightwave Technol.*, DOI: 10.1109/50.60571, 1990.

[35] J. Morgado and A. Cartaxo, "Assessment of laser noise influence on direct-detection transmission system performance," *J. Lightwave Technol.*, DOI: 10.1109/JLT.2003.809571, 2003.

[36] J. Rebola, T. Alves, and A. Cartaxo, "Outage probability due to intercore crosstalk from multiple cores in short-reach networks," *Photon. Technol. Lett.*, vol. 33, no. 6, pp. 281-284, 2021.